A Journey of Trains of Droplets in Droplet-Based Microfluidic Devices

Hun Lee, Linfeng Xu, and Kwang W. Oh

Abstract— **In this paper, we propose a microfluidic platform toseparate magnetic particles with a constant volumetric flow condition. In order to realize this architecture, three main functions for a droplet manipulation based system are integrated into a single device: synchronization of droplets by matching a location of droplets; lateral electro-coalescence; and magnetic particle manipulation. For an optimized condition of this device, a droplet generation was controlled by varying a droplet size at a fixed flow rate ratio 0.86. The electro-coalescence efficiency and maximum throughput are investigated at a given flow rate condition.**

I. Introduction

Droplet-based microfluidic devices have great potential for high-throughput applications in biological and chemical studies [1]. The main advantage of droplet based microfluidic devices is that they enable all molecular reactions to occur in a confined small volume of a single droplet so that the reactions occur without cross-comtamination between droplets and the surrounding environment [2-5]. Moreover, it provides a strong reduction of reagent volume and reation time because the dimensional scaling effect allows for rapid heat and mass transfer in the droplets [6]. In addition, with the manipulation of droplets, the reagents of interest can be transported, merged, mixed, and analyzed as a micro-reactor effectively and quickly [7].

In the past decade, magnetic particles have been used as a solid support in a microfluidic device since the magnetic particles can easily be manipulated in a fluidic environment by magnetic fields [8]. It does not require any sophisticated or expensive system to manipulate them. Moreover, they offer a high surface-to-volume ratio resulting in an increased sensitivity of fluorescence signal on the surface of magnetic particles due to large binding capacity for efficient biological reactions [9]. However, the ability to apply droplet-based microfluidic devices to high-throughput magnetic particle-based assays is extremely promising but has been barely attempted.

Previously, there have been great efforts in developing various unit functions to perform cell encapsulation [10,11], manipulation of droplets (e.g., merging [12,13], mixing [14] and sorting [15]), on-chip incubation [16], and generation of multiple reagents [17]. Furthermore, the droplet-based microfluidic devices are being successfully commercialized by Raindance Technologies. In conventional droplet-based microfluidic technologies, additive functions (e.g., particle/cell encapsulation, sequential fusion, rapid mixing, dilution) are well understood and demonstrated. However, subtractive functions (e.g., in-droplet particle separation) have been limited, unlike the continuous-flow and electrowetting-based microfluidic device (Fig. 1). In these devices reagents can be easily added with additional contents or diluted with additional buffers by droplet fusion (Fig. 1a), but cannot be subtracted or separated into another droplet for the downstream on-chip or off-chip analysis (Fig. 1b).

In order to overcome these technical challenges, we developed a droplet-based magnetic particle separation module by combining three unit functions: parallel synchronization of two trains of droplets; lateral electro-coalescence; magnetic particle manipulation. For the first unit function, we used a passive droplet synchronization method that was already developed from our group [18]. The channel network consists of two main channels. One channel for the droplets to flow through, while the other, is an interconnection channel that allows the oil carrier fluid to flow. This is a simple method for passive droplet synchronization of two trains of droplets by a pressure-talk between the droplets. For the second unit function, ITO electrodes were deposited on a glass substrate to apply electric field which can lead to instability of the interfaces between the water phase and the oil phase [19]. Thus, the droplets merge together once they come in contact with each other. The key idea in this device is that the electro-coalescence occurs in a lateral way, which enables the magnetic particle separation. The lateral electro-coalescence

(a) Conventional droplet-based additive function
Sequential fusion + Rapid mixing + Dilution

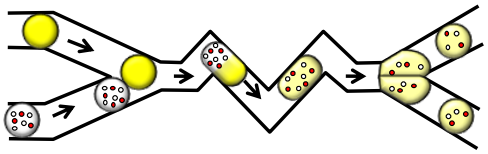

(b) Proposed droplet-based subtractive function
Parallel fusion + Controlled mixing + Separation

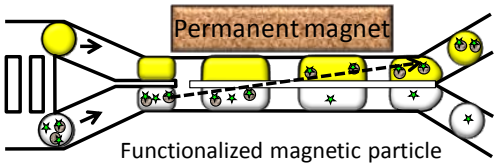

Fig. 1 (a) The conventional droplet-based additive function with sequential fusion, rapid mixing and dilution of paired-droplets due to chaotic advection by recirculating flows (b) The proposed droplet-based subtractive function.

This work was supported by grants from NSF (ECCS-1002255 and ECCS-0736501).

H. Lee, L. Xu, and K. W. Oh are with the Department of Electrical Engineering, State University of New York at Buffalo, Buffalo, NY 14260, USA (e-mail: hlee24@buffalo.edu, linfengx@buffalo.edu, and kwangoh@buffalo.edu).

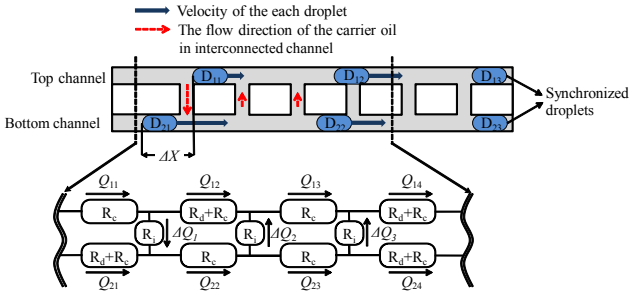

Fig. 2 Schematic view for droplet synchronization where Q_{xy} is the volumetric flow rate for each channel section (x = 1 and x = 2 refer to the top and bottom channels, and y refers to the section number of the channel), ΔQ represents volumetric flow rate for the interconnected channels, and R_i, R_c and R_d represent the hydraulic resistance values for the interconnected channels, for the section of the main channels and across the generated droplets, respectively [18].

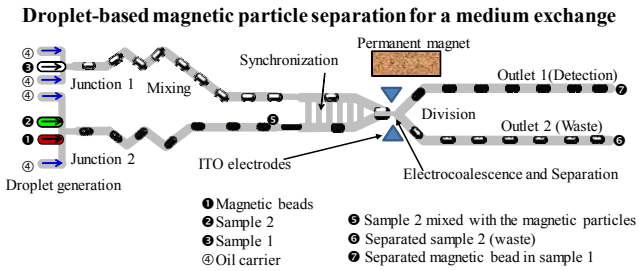

Fig. 3 Schematic workflow of the proposed droplet-based microfluidic device for magnetic particle-based assays including a washing function by a series of procedures. The droplet generation, mixing, parallel synchronization, lateral electrocoalescence, and magnetic particle separation were sequentially conducted for the simple streptavidin-biotin immunoassay.

of the synchronized droplets occurs at the beginning of an X-shape junction in which ITO electrodes are placed. For the third unit function, the magnetic particles are manipulated using a magnetic field created from a permanent magnet which allows them to be separated from one droplet to the other: one contains almost all of the magnetic particles and the other is including a waste of sample without magnetic particles.

In this paper, using the three main functions, we demonstrate magnetic particle-based in-droplet separation with constant volumetric flow in droplet-based microfluidic platform. The droplet generation, mixing, synchronization, electro-coalescence, in-droplet magnetic particle separation and splitting are sequentially performed on the microfluidic device to achieve the subtractive droplet-based separation. As a result, we exchange the surrounding medium of magnetic particles within a droplet by performing the magnetic particle separation. We believe that this approach has a great potential for practical use due to the unique magnetic particle-based in-droplet separation. In addition, this method will be used to perform a washing step to remove an unbound reagent in immunoassay.

II. Working Principle

A. Synchronization of droplets in a channel network

The droplets passing through the two main channels, the top and bottom channel, cause a pressure difference between them. However, the pressure difference can be diminished by a cross flow of carrier oil through the interconnection network as the pressure in each channel was balanced automatically (Fig. 2). For example, if there is a phase difference (ΔX) between the droplets (D_{11} and D_{21}), they lead to the pressure difference between the top and bottom channels, temporally blocking the channels. The droplet (D_{11}) increases hydraulic resistance at the top channel, which allows the volumetric flow of the carrier oil to pass through the interconnection channel: there is no way for oil to flow anywhere else other than the first interconnection channel. Thus the velocity of the droplet in the top channel is slower compared to the initial velocity: $Q_{11} > Q_{12}$. On the other hand, the volumetric flow of the carrier oil (Q_{22}) is increased by ΔQ_1, resulting in an increased velocity of the droplet (D_{21}) in the bottom channel.

Consequentially, the ΔX is diminished by the balanced pressure, $Q_{14} = Q_{24}$, between the main channels so that the synchronization of droplet can be achieved without any active sources [18]. By using this mechanism, we have designed the railroad-like channel network that allows the lateral electrocoalescence of droplets.

B. Lateral electrocoalescence

The droplet synchronization unit enables the two trains of the droplets to be merged laterally. The electrostatic forces applied from the ITO electrodes at an entrance of the X-shape separation junction. The electric field can cause the interface between the oil phase and the water phase to be unstable so that they can easily be merged. To ensure successful electro-coalescence, we applied a DC voltage of 50 V_{DC}.

C. Magnetic particle manipulation

In order to separate the magnetic particles within the droplets, the magnetic field was applied near the X-shape junction. The magnetic force, F_{mag}, on the magnetic particles is defined by

$$F_{\mathrm{mag}} = \frac{1}{2}\frac{V\Delta\chi}{\mu_0}\nabla B^2$$

where V is the volume of the magnetic particles, μ_0 is the permeability of free space, B is the magnetic field, and $\Delta\chi$ is the susceptibility of the magnetic particles in a surrounding medium. In the present device, the permanent magnet is located 1 mm away from the channel [8]. The magnetic fields are applied perpendicular to a direction of flow.

A total workflow of the proposed droplet-based microfluidic device for the in-droplet magnetic particle separation is illustrated in Fig. 3. The droplet-based separation is performed by a series of the following procedures. Two trains of droplets are generated at droplet generation junctions 1 and 2 at the given flow rate condition (see Table 1). The droplet generated at junction 1 represents a droplet with sample 1 (③). For a droplet at junction 2, the sample 2 (②) and magnetic particles (①) are co-infused. The sample 2 droplets are fully mixed in a serpentine channel region. The sample 1 and sample 2 droplets are introduced into a ladder-like channel network to make them

synchronized. The two parallel-synchronized droplets are merged at an entrance of the X-shape separation junction by an electric field, which can cause the interface between the oil and water to be unstable. At this X-shape junction, the magnetic particles are traversed to the sample 1 (top of the merged droplet) by an externally applied magnetic field, leaving the sample 2 (bottom of the merged droplet). Subsequently, the merged droplet is split into two daughter droplets at the X-junction: sample 1 containing the majority of magnetic particles and sample 2 devoid of the magnetic particle. As a result, the surrounding medium of magnetic particle was exchanged from the sample 1 and sample 2.

III. Method and Materials

A. Device fabrication

We used a conventional soft-lithography technique to fabricate SU-8 mold for the microfluidic channels. As a substrate, the 3 inch silicon wafer was used. The thin oxide layer grown in natural condition on the wafer was removed by BHF (buffered hydrofluoric acid) to increase the adhesive force between SU-8 and wafer at room temperature for 5 min. Afterwards, the wafer was rinsed by acetone, methanol and distilled water, and then dried with filtered nitrogen gas. After dehydration of the wafer on a hot plate at 120 °C for 5 min, the SU-8 2050 was deposited by spin coating process with target thickness (50 μm) using a spin processer. The soft bake, UV exposure, post exposure bake, and development were carried out sequentially.

Indium tin oxide (ITO) was formed using lift-off process on a glass substrate as the electrodes. A positive photoresist (S1818) was patterned on the glass substrate by the lithography to define the position of electrodes. The ITO electrodes (300 nm) were deposited on the substrate by DC sputter.

A pre-polymer of PDMS and curing agent were prepared and mixed in a 10:1 (wt/wt) ratio. After removing the bubbles generated during the mixing, the mixture of PDMS poured on the fabricated SU-8 master mold and cured at 65 °C for 30 min. The PDMS replica was punched for inlets and outlets and then bonded irreversibly by exposing O_2 plasma on the ITO patterned glass substrate.

B. Materials and operation

To apply magnetic field, a permanent magnet (12.7 × 3.2 × 3.2 mm^3, Emovendo Magnets & Elements, Petersburg, WV, USA) with a rectangular shape was used. Mineral oil (M8410, Sigma-Aldrich) with 2% Span-80 (S6760, Sigma-Aldrich) was used as the oil carrier flow. To change the surface property of PDMS channel from hydrophilic and hydrophobic surface coating material (Aquapel, 47100) was used. The magnetic beads (2.8 μm diameter, Dynabeads M-270 streptavidin, Invitrogen) were mixed in deionized water, giving ~ 5 × 10^8/ml concentration. To generate the electric field to merge the droplets the DC voltage was supplied by a high-voltage source (HVS448-1500) connected to a computer controller to generate an electric field through ITO electrodes. The inlets of microfluidic device were connected by polyethylene tube. To generate the constant volumetric flow, a syringe pump (KDS100W) was used. To capture and analyze images, a CMOS camera equipped with a microscope was used.

TABLE 1. Flow rate conditions to generate the droplets at the junctions 1 and 2.

Flow rate condition	Junction 1		Junction 2		
	Q_o ④ (μl/h)	Q_w ③ (μl/h)	Q_o ④ (μl/h)	Q_w ① (μl/h)	Q_w ② (μl/h)
A	35	30	35	15	15
B	70	60	70	30	30
C	105	90	105	45	45

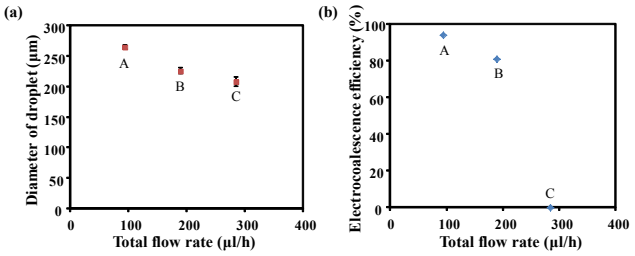

Fig. 4 (a) The diameter of droplet as a function of total flow rate. (b) Electrocoalescence efficiency as a function of total flow rate.

IV. Result and Discussion

As the device has two flow focusing junctions to generate droplets, two trains of droplets can be independently generated at given condition listed in Table 1. In this device, it is critical to optimize the droplet size for stable the synchronization and electro-coalescence. In order to find out optimized condition, the water (Q_w) and oil (Q_o) flow rates were adjusted. The diameter of droplets was varied from 208 μm to 265 μm as shown in Fig. 4a.

To ensure successful electro-coalescence, we applied a DC voltage of 50 V_{DC} to the ITO electrodes. The electro-coalescence efficiency, defined by the number of successfully merged droplets over the total number of generated droplets, was plotted as a function of total flow rate where the flow rate ratio ($Q_{ratio} = Q_w / Q_o$) to generate droplets was fixed at 0.86.

In the case A, we applied the sample 1 solution at 60 μl/h and oil 35 μl/h into junction 1. The corresponding diameter of droplet and total flow rate ($Q_{total} = Q_w + Q_o$) were 265 μm and 95 μl/h. The maximum efficiency of 94% was achieved at the total flow rate of 95 μl/h. However, in the case C, the diameter of droplet was 208 μm and no electro-coalescence occurred at all at the X-junction as shown in Fig. 4b. The X-junction is designed to facilitate the droplets merging at the end of the interconnection channels. If small droplets meet at the X-junction they cannot get touch each other. The thin

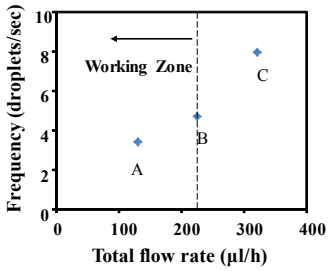

Fig. 5 The droplet generation frequency as a function of total flow rate. The working zone is indicated by an arrow. In the case C, the electrocoalescence efficiency was zero due to the small size of droplets.

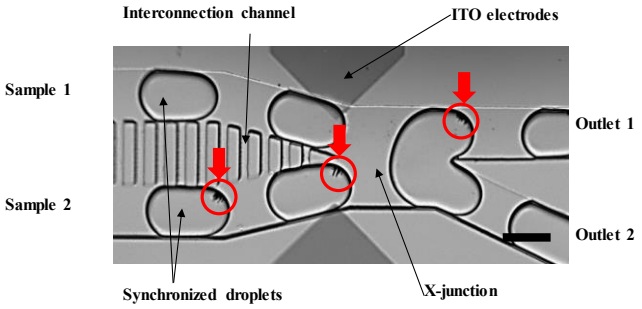

Fig. 6 Photograph image to show the manipulation of the magnetic particles within the droplets. The magnetic particles are already concentrated to one side of the droplet as they approach the permanent magnet so that they are extracted into the sample 1 droplet. Circles with red arrows indicate the clusters of the magnetic particles moving from sample 2 to sample 1. The scale bar is 200 μm.

membrane of oil carrier flow will present between the two droplets preventing them to be merged. This failure occurred due to the small size of droplet. Fig. 5 shows droplet generation frequency as a function of total flow rate. The maximum frequency was 4.7 droplets/sec.

We added magnetic particles in the sample 2 droplets to study in-droplet magnetic particle separation. Fig. 6 shows the photograph of the in-droplet magnetic particle manipulation. The red arrows are indicating the clusters of the magnetic particles. In this experiment, the optimized condition (case A) was used for the stable in-droplet separation. A permanent magnet was located in the vicinity of the X-junction where the in-droplet magnetic particle separation occurred perpendicular to the direction of flow. The magnetic field force was calculated to be about 320 mT at the junction. As the magnetic particles approached near the magnetic fields, they were magnetized, locally in the form of clusters in each droplet. Under the magnetic fields, the clusters were concentrated towards the magnet, so that the clustered magnetic particles easily traversed to the sample 1 droplet for medium exchange. As a result, the droplet-based magnetic particle separation was successfully achieved by extracting the magnetic particle from the sample 2 droplet to the sample 1 droplet.

V. Conclusion

In this paper, we suggest the droplet-based microfluidic device to exchange the surrounding medium of magnetic particle for biological applications by separating the magnetic particles from one droplet to another. We investigate the optimal condition, varying water and oil flow rates. The successful electro-coalescence of 94% was achieved and the maximum droplet generation frequency was 4.7 droplets/sec. The proposed method will enable magnetic particle-based immunoassay involving a washing step in a continuous flow droplet-based microfluidic platform.

References

[1] S. Y. Teh, R. Lin, L. H. Hung, and A. P. Lee, "Droplet microfluidics," *Lab Chip*, vol. 8, pp. 198-220, 2008.

[2] A. R. Abate, T. Hung, P. Mary, J. J. Agresti, and D. A. Weitz, "High-throughput injection with microfluidics using picoinjectors," *P. Natl. Acad. Sci. USA*, vol. 107, pp. 19163-19166, 2010.

[3] D. R. Link, S. L. Anna, D. A. Weitz, and H. A. Stone, "Geometrically mediated breakup of drops in microfluidic devices," *Phys. Rev. Lett.*, vol. 92, pp. 054503, 2004.

[4] L. Mazutis, A. F. Araghi, O. J. Miller, J. C. Baret, L. Frenz, A. Janoshazi, V. Taly, B. J. Miller, J. B. Hutchison, D. Link, A. D. Griffiths, and M. Ryckelynck, "Droplet-Based Microfluidic Systems for High-Throughput Single DNA Molecule Isothermal Amplification and Analysis," *Anal. Chem.*, vol. 81, pp. 4813-4821, 2009.

[5] V. Taly, B. T. Kelly, and A. D. Griffiths, "Droplets as microreactors for high-throughput biology," *Chembiochem*, vol. 8, pp. 263-272, 2007.

[6] D. Janasek, J. Franzke, and A. Manz, "Scaling and the design of miniaturized chemical-analysis systems," *Nature*, vol. 442, pp. 374-380, 2006.

[7] G. M. Whitesides, "The origins and the future of microfluidics," *Nature*, vol. 442, pp. 368-373, 2006.

[8] N. Pamme, "Magnetism and microfluidics," *Lab Chip*, vol. 6, pp. 24-38, 2006.

[9] S. A. Peyman, A. Iles, and N. Pamme, "Mobile magnetic particles as solid-supports for rapid surface-based bioanalysis in continuous flow," *Lab Chip*, vol. 9, pp. 3110-3117, 2009.

[10] J. Clausell-Tormos, D. Lieber, J. C. Baret, A. El-Harrak, O. J. Miller, L. Frenz, J. Blouwolff, K. J. Humphry, S. Koster, H. Duan, C. Holtze, D. A. Weitz, A. D. Griffiths, and C. A. Merten, "Droplet-based microfluidic platforms for the encapsulation and screening of mammalian cells and multicellular organisms," *Chem. Biol.*, vol. 15, pp. 875-875, 2008.

[11] J. F. Edd, D. Di Carlo, K. J. Humphry, S. Koster, D. Irimia, D. A. Weitz, and M. Toner, "Controlled encapsulation of single-cells into monodisperse picolitre drops," *Lab Chip*, vol. 8, pp. 1262-1264, 2008.

[12] K. Ahn, J. Agresti, H. Chong, M. Marquez, and D. A. Weitz, "Electrocoalescence of drops synchronized by size-dependent flow in microfluidic channels," *Appl. Phys. Lett.*, vol. 88, 2006.

[13] M. Chabert, K. D. Dorfman, and J. L. Viovy, "Droplet fusion by alternating current (AC) field electrocoalescence in microchannels," *Electrophoresis*, vol. 26, pp. 3706-3715, 2005.

[14] F. Sarrazin, L. Prat, N. Di Miceli, G. Cristobal, D. R. Link, and D. A. Weitz, "Mixing characterization inside microdroplets engineered on a microcoalescer," *Chem. Eng. Sci.*, vol. 62, pp. 1042-1048, 2007.

[15] K. Ahn, C. Kerbage, T. P. Hunt, R. M. Westervelt, D. R. Link, and D. A. Weitz, "Dielectrophoretic manipulation of drops for high-speed microfluidic sorting devices," *Appl. Phys. Lett.*, vol. 88, 2006.

[16] H. Song, J. D. Tice, and R. F. Ismagilov, "A microfluidic system for controlling reaction networks in time," *Angew. Chem. Int. Edit.*, vol. 42, pp. 768-772, 2003.

[17] J. Q. Boedicker, L. Li, T. R. Kline, and R. F. Ismagilov, "Detecting bacteria and determining their susceptibility to antibiotics by stochastic confinement in nanoliter droplets using plug-based microfluidics," *Lab Chip*, vol. 8, pp. 1265-1272, 2008.

[18] B. Ahn, K. Lee, H. Lee, R. Panchapakesan, and K. W. Oh, "Parallel synchronization of two trains of droplets using a railroad-like channel network," *Lab Chip*, vol. 11, pp. 3956-3962, 2011.

[19] H. Gu, M. H. G. Duits, and F. Mugele, "Droplets Formation and Merging in Two-Phase Flow Microfluidics," *Int. J. Mol. Sci.*, vol. 12, pp. 2572-2597, 2011.